This article has been accepted for publication in a future issue of this journal, but has not been fully edited. Content may change prior to final publication. Citation information: DOI 10.1109/TIA.2015.2510507, IEEE Transactions on Industry Applications

Maximum Power Point Tracking Control of IPMSG Incorporating Loss Minimization and Speed Sensorless Schemes for Wind Energy System

M. Nasir Uddin, *Senior Member IEEE*, and Nirav Patel

Department of Electrical Engineering
Lakehead University
Thunder Bay, Ontario P7B 5E1, Canada
E-mails: muddin@lakeheadu.ca, npatel4@lakeheadu.ca

***Abstract* – In the variable-speed generation system, the wind turbine can be operated at maximum power operating points by adjusting the shaft speed optimally. This paper presents a novel maximum power point tracking (MPPT) based control of interior permanent magnet synchronous generator incorporating loss minimization algorithm. In the proposed method, without requiring the knowledge of wind speed, air density or turbine parameters, MPPT algorithm generates optimum speed command for speed control loop of vector controlled machine side converter. The MPPT algorithm uses the estimated active power output of the generator as its input and generates command speed so that maximum power is transferred to the dc-link. The proposed control system also incorporates a loss minimization algorithm to minimize the losses in the generator and hence, to improve the efficiency of the wind energy conversion system. A speed sensorless scheme is also incorporated to increase the reliability of the system. The performance of the proposed adaptive MPPT control of wind generator incorporating loss minimization and speed sensorless schemes is tested in both simulation and experiment at variable wind speed conditions.**

***Index Terms*— Wind energy, maximum power point tracking control, Loss minimization algorithm, speed sensorless control, IPM synchronous generator.**

I. INTRODUCTION

The popularity of renewable energy has experienced significant growth recently due to the foreseeable exhaustion of conventional fossil fuel power generation methods and increasing realization of the adverse effects that conventional fossil fuel power generation has on the environment. Among the renewable energy sources, wind energy has received great attention as a safe and clean renewable power source [1]-[7].

A typical block diagram of direct-drive wind energy conversion system (WECS) is shown in Fig. 1. Recently, the interior permanent magnet synchronous machine (IPMSM) has received much attention in direct-drive wind energy application because of its several advantages such as, high efficiency, higher power density, less maintenance, low noise and robustness. A direct drive variable speed wind turbine can be based on a surface type or interior type permanent magnet synchronous generator (IPMSG). However, an IPMSG can produce more energy as compared to that of surface type permanent magnet synchronous generator (SPMSG) [7]-[9]. Despite many advantages the control of IPMSG is complicated due to magnetic saliency and its nonlinear coupling between d-q axis currents. Moreover, the inductance parameters of IPMSM vary with the magnetic saturation that affects the performance of the generator in both transient and steady-states.

Researchers have been developing several techniques for maximum power point tracking (MPPT) operation of IPMSG so that the maximum power can be transferred from wind to the dc link of the input side converter of the WECS [1,5,9-11]. Several types of control schemes such as duty cycle control, look up table for optimum rotor speed, optimum tip speed ratio (TSR) have been proposed to improve the performance of wind power extraction [10]-[12]. However, these schemes depend on the characteristics of wind turbine (WT) either before or during execution. Moreover, the WT components tend to change their characteristics over the time. Control strategy independent of the WT characteristics, such as perturbation and observation (PO) method is very flexible and accurate [13-15]. Optimum power search algorithm proposed in [3] tracks peak power points in power curve (P-ω) corresponds to, $\frac{dP}{d\omega} = 0$. In [5] and [15] neural network based MPPT algorithms for SPMSG are proposed. However, the control of SPMSG is easier than that of IPMSG [3-5]. Furthermore, in most of the published works on WECS the loss minimization in the generator was ignored [1-7,9-15]. But the machine loss minimization is an important issue to improve the efficiency of WECS. Again, the removal of rotor position sensor for the generator is a crucial issue for reliable operation of WECS as the sensor is vulnerable for electromagnetic noise in hostile environments and has a limited temperature range. For PM machines rated up to 10kW the cost of an encoder is below 10% of the machine manufacturing cost. So, the cost of replacing the sensor may not be an issue. But it is hard to replace the sensor due to the limited accessibility. Thus, the elimination of the electromechanical sensors reduces the hardware costs, the installation complexity of the system (because of associated wiring), decreases the system inertia, increases the robustness and the reliability and reduces obviously the noise sensitivity of the WECS [14-18]. Among different types of rotor speed estimation techniques, the model reference adaptive system (MRAS) scheme offers simpler implementation and require less computational effort as compared to other methods [17-22]. Thus, the MRAS is utilized in this work for rotor position estimation of IPMSG. Moreover, the integration of

0093-9994 (c) 2015 IEEE. Personal use is permitted, but republication/redistribution requires IEEE permission. See http://www.ieee.org/publications_standards/publications/rights/index.html for more information.

This article has been accepted for publication in a future issue of this journal, but has not been fully edited. Content may change prior to final publication. Citation information: DOI 10.1109/TIA.2015.2510507, IEEE Transactions on Industry Applications

MPPT scheme with loss minimization and speed sensorless schemes for IPMSG has never been reported. The control strategy to minimize the machine losses can be divided into two categories: a) search controller (SC), b) loss-model-based controller (LMC). The basic principle of the SC is to measure the input power and then iteratively search for the flux level (or its equivalent variables) until the minimum input power is detected for a given torque and speed. Important drawbacks of the SC are the slow convergence and torque ripples. The model-based controller computes losses by using the machine model and selects a flux level that minimizes the losses [23-25]. LMC is fast and does not produce torque ripple.

Therefore, in this paper, a novel adaptive MPPT algorithm incorporating an LMC and speed sensorless schemes is developed to transfer maximum power from WT to the dc-link. The MPPT algorithm generates the optimum reference speed for IPMSG based on the output power of the generator. A motor model based loss minimization algorithm (LMA) is integrated with the MPPT to optimize the efficiency of the WECS [23]. The LMA generates the optimum d-axis current i_d, which controls the flux to minimize the electrical losses (i.e., copper and iron losses).

In order to verify the effectiveness of the proposed IPMSG based WECS, a simulation model is developed using MATLAB-Simulink. The proposed system is also implemented in real-time using DSP board DS1104 for a 5 hp IPMSG. It is found from the results that proposed control techniques can transfer maximum power while maintaining high efficiency, controllability and accurate speed estimation of the generator.

II. Wind Energy Conversion System (WECS)

A. Modeling of Wind Turbine

A typical variable speed direct-drive WECS is shown in Fig.1.The area inside the dotted line of WECS shows the scope of this paper. A variable speed WT driven IPMSG is connected to the DC link through controlled rectifier. As this system doesn't use gear box, it is called direct-drive WECS. Using the mechanical torque of WT, the IPMSG produces 3-phase AC power which is converted to DC power using controlled rectifier.

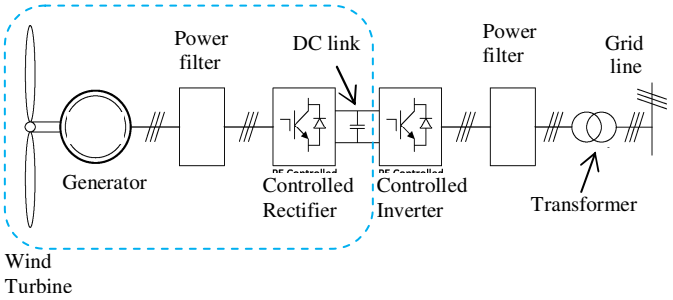

Fig. 1 Typical variable speed WECS.

The mechanical power and torque that WT extracts from the wind is calculated by the following equations [12]:

$$P_m = \tfrac{1}{2}\rho A v_s^3 C_P(\lambda,\beta) = f(v_s,\omega_t) \quad (1)$$

$$T_m = \frac{P_m}{\omega_s} \quad (2)$$

$$C_P = \frac{1}{2}\left(116\frac{1}{\zeta} - 5\right)e^{\left(-21\frac{1}{\zeta}\right)} \quad (3)$$

$$\frac{1}{\zeta} = \frac{1}{\lambda + 0.08\beta} - \frac{0.035}{1+\beta^3} \text{ and } \lambda = \frac{\omega_s R}{v_s} \quad (4)$$

where, P_m - power in watts, ρ-Air density (1.2kg/m³ @ sea level and 20° C), A- Swept area of the turbine blades (m²), v_s= Wind speed (m/s), C_p- Wind turbine power coefficient, β - pitch angle =0, ω_s- angular velocity of turbine (rad/s), R - rotor radius (m), and λ- tip speed ratio (=blade tip speed/wind speed). A real wind speed can be defined as [16]:

$$v_s(t) = v_b(t) + v_r(t) + v_g(t) + v_n(t) \quad (5)$$

where, V_b= base wind component, V_r = ramp wind component, V_g = gust wind component, and V_n = base noise wind component. In wind energy conversion system output power is maximum at particular rotor speed for a given wind speed. Fig. 2 shows the power coefficient C_P vs tip speed ratio (TSR), λ. The maximum C_p that can be obtained for the specific TSR is 0.4655. To further explain this concept, Fig. 3 shows the typical WT and generator power curve at different rotor speed for different wind velocities. Maximum turbine power, $P_{m\ max}$ and generator power, $P_{e\ max}$ are the maximum power points at different rotor speed with changing wind. It is desired that the maximum power controller follows that generator power curve at variable wind speed.

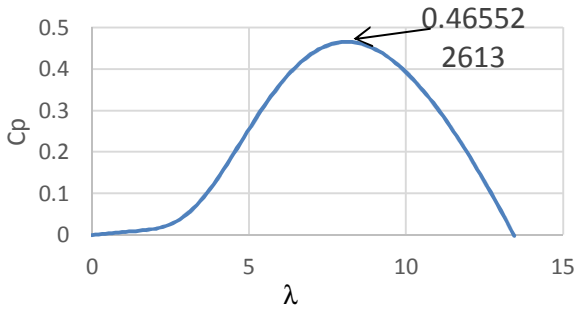

Fig. 2 C_P as a function of λ at different wind velocities.

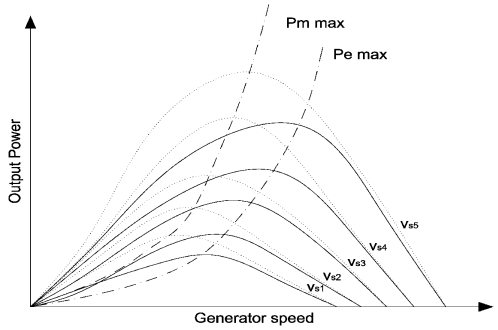

Fig. 3 Power-Speed characteristics at various wind velocities ('….' -turbine power; '___'-generator power.

0093-9994 (c) 2015 IEEE. Personal use is permitted, but republication/redistribution requires IEEE permission. See http://www.ieee.org/publications_standards/publications/rights/index.html for more information.

This article has been accepted for publication in a future issue of this journal, but has not been fully edited. Content may change prior to final publication. Citation information: DOI 10.1109/TIA.2015.2510507, IEEE Transactions on Industry Applications

B. Mathematical Model of IPMSM

Conventionally, the IPM synchronous machine can be represented mathematically in d-q synchronous rotating frame as [1]:

$$v_q = i_q R_s + \frac{d\psi_q}{dt} + \omega\psi_d \tag{6}$$

$$v_d = i_d R_s + \frac{d\psi_d}{dt} - \omega\psi_q \tag{7}$$

where, v_d, v_q are d-q axis voltages and i_d, i_q are d-q axis currents, ψ_d, ψ_q are d-q axis flux linkages, respectively and R_s is the stator resistance per phase; ω (= $P\omega_s$) is electrical angular speed and P is the number of pole pairs of IPMSM. The d-q axis flux linkages, ψ_d and ψ_q can be written as,

$$\psi_d = L_d i_d + \psi_m \quad \text{and,} \quad \psi_q = L_q i_q \tag{8}$$

where, ψ_m is the magnetic flux linkage, and L_d, L_q are d-q axis inductance, respectively.

When using lumped mass model as given in equation below for WT generator shaft system, the motion equation of IPMSG can be expressed as:

$$J\frac{d\omega_r}{dt} = T_m - T_e - B_m\omega_s \tag{9}$$

where, J - total moment of inertia of the wind turbine and generator (Kg.m^2), B_m- damping coefficient (Kg.m^2/s), T_m- input mechanical torque (Nm) given by (2). In the above mathematical model, core loss is not incorporated and hence not suitable to develop loss minimization algorithm.

C. Model Based Loss Minimization Algorithm of IPMSM

The d-q axis equivalent circuits of interior permanent magnet synchronous machine incorporating stator copper and core losses are shown in Fig. 4. The core loss, which is caused by hysteresis and eddy currents, is represented by an equivalent core-loss resistance, R_c. Considering this resistance, the IPMSM can be represented mathematically in d-q synchronous rotating frame as:

$$\begin{bmatrix} v_d \\ v_q \end{bmatrix} = R_s \begin{bmatrix} i_{de} \\ i_{qe} \end{bmatrix} + \left(1 + \frac{R_s}{R_c}\right)\begin{bmatrix} v_{de} \\ v_{qe} \end{bmatrix} \tag{10}$$

$$\begin{bmatrix} v_{de} \\ v_{qe} \end{bmatrix} = \begin{bmatrix} 0 & -\omega\sigma L_d \\ \omega_r L_d & 0 \end{bmatrix}\begin{bmatrix} i_{de} \\ i_{qe} \end{bmatrix} + \begin{bmatrix} 0 \\ \omega\psi_m \end{bmatrix} \tag{11}$$

$$i_{cd} = -\frac{\omega\sigma i_{qe} L_d}{R_c}, \; i_{cq} = \frac{\omega(\psi_m + i_{de} L_d)}{R_c} \tag{12}$$

$$i_{de} = i_d - i_{cd}, \qquad i_{qe} = i_q - i_{cq} \tag{13}$$

where, i_{de} and i_{qe} are d-axis demagnetizing and q-axis torque generating currents, respectively, i_{cd} and i_{cq} are d-q axis core loss currents, and saliency ratio, $\sigma = L_q/L_d$. Copper and core losses are the two controllable losses in IPMSM. Eddy current losses are caused by the flow of induced currents inside the stator core and hysteresis losses

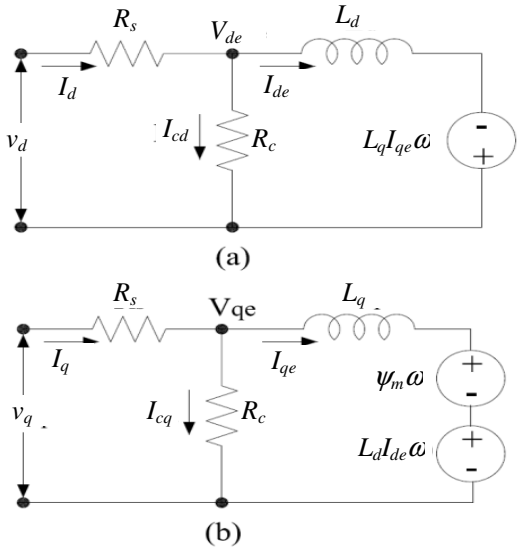

Fig.4 Equivalent circuits of IPMSM: (a) d-axis, (b) q-axis.

are caused by the continuous variation of flux linkages and frequency of the flux variation in the core. On the other hand copper loss, P_{Cu} is due to current flow through the stator windings. Based on Eqns. (12), (13) and Fig. 4 the copper loss P_{Cu}, iron loss P_{Fe}, and efficiency η are expressed as follows:

$$\begin{aligned} P_{cu} &= R_s(i_d^{\,2} + i_q^{\,2}) \\ &= R_s\left\{i_{de} - \left(\frac{\omega\sigma L_d i_{qe}}{R_c}\right)\right\}^2 + R_s\left\{i_{qe} + \left(\frac{\omega(\psi_r + L_d i_{de})}{R_c}\right)\right\}^2 \end{aligned} \tag{14}$$

$$P_{Fe} = R_c(i_{cd}^{\,2} + i_{cq}^{\,2}) = R_c\left(\frac{\omega\sigma L_d i_{qe}}{R_c}\right)^2 + R_c\left(\frac{\omega^2(\psi_r + L_d i_{de})}{R_c}\right)^2 \tag{15}$$

$$P_E = P_{cu} + P_{Fe} \qquad P_L = P_M + P_E \qquad \eta = \frac{P_{out}}{P_{out} + P_L}100\,\% \tag{16}$$

where, P_L- total loss, P_M- mechanical loss, P_E- electrical loss, P_{out}- dc-link power and η is the overall efficiency of the WECS. In order to find the core loss resistance, R_c at rated load and speed first, the iron loss P_{Fe} is calculated by subtracting mechanical loss P_{mech}, copper loss P_{cu}, and rated output power P_{out} from the rated input power P_{in}. Then the R_c is calculated from the expression (15). The core loss resistance, R_c changes with operating condition as it is a function of air-gap flux and frequency. But for simplicity in this work it is assumed constant. The electromagnetic developed torque is given by,

$$T_e = \frac{3P}{2}\{\psi_r i_{qe} + (L_d - L_q) i_{de} i_{qe}\} \tag{17}$$

As seen that the torque is nonlinear with i_{de} and i_{qe}. The first part is the magnetic torque and the second part is the reluctance torque. The reluctance torque is absent in surface mounted PMSG as $L_d = L_q$.

Both search based and models based LMAs have been used in vector-controlled IPMSM drives [23]. The search based

0093-9994 (c) 2015 IEEE. Personal use is permitted, but republication/redistribution requires IEEE permission. See http://www.ieee.org/publications_standards/publications/rights/index.html for more information.

This article has been accepted for publication in a future issue of this journal, but has not been fully edited. Content may change prior to final publication. Citation information: DOI 10.1109/TIA.2015.2510507, IEEE Transactions on Industry Applications

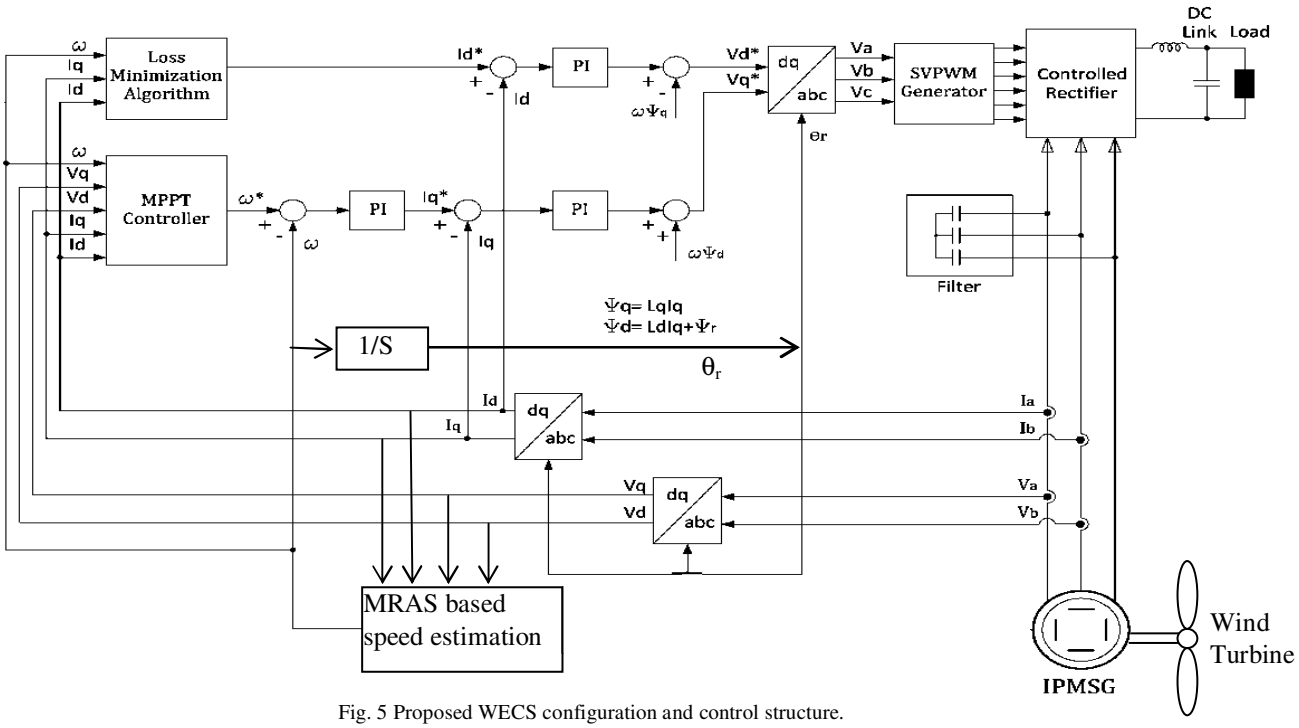

Fig. 5 Proposed WECS configuration and control structure.

loss minimization technique has its own advantages such as insensitivity to parameter variations caused by temperature and magnetic saturation. In the search based technique the flux is decremented in a stepwise manner until the minimum input power of the IPMSM is detected and thus, it ensures minimum loss condition. However, the search based loss minimization is slow in convergence.

In model based loss minimization the optimum d-axis current (i_d^*), which provides the minimum electrical loss, is derived based on motor model. The optimum i_d^* can be found by partially differentiating P_E with respect to flux component of d-axis current, i_{de} and setting it to zero as [22], $\frac{\partial P_E}{\partial i_{de}} = 0.$

Assuming T_e, ω= constant as wind won't have sudden change over short period of time and hence, loss minimization condition is obtained as,

$$MN - T_e^2 O = 0 \tag{18}$$

where,

$$M = P_n^2 \{R_s R_c^2 i_{de} + \omega^2 L_d (R_s + R_c)(L_d i_{de} + \psi_r)\} \tag{19}$$

$$N = [\psi_r + (1-\sigma) L_d i_{de}]^3 \tag{20}$$

$$O = \{R_s R_c^2 + (R_s + R_c)(\omega\sigma Ld)^2\}(1-\sigma) Ld \tag{21}$$

For given torque T_e and speed ω the optimal i_d^*, is derived from (19)-(22) as,

$$i_d^* = -V^{-1}(W i_{de}^2 + X i_{de}^3 + Y i_{de}^4 - Z) \tag{22}$$

where, V, W, X, Y and Z are given by,

$$V = (\psi_r^3 \lambda + \omega^2 - 2 i_{qe}^2 \sigma^2 \psi_r L_d^4 \alpha\lambda\omega^2 (R_s + R_c) \tag{23}$$

$$W = 3((\omega^2 L_d^3 (R_s + R_c)\psi_r^2 \alpha)(1+\alpha) + L_d \psi_r^2 \alpha \lambda) - 2 i_{qe}^2 \sigma^2 \psi_r L_d^5 \alpha^3 \lambda \omega^2 (R_s + R_c) \tag{24}$$

$$X = 3 L_d^2 \psi_r \alpha^2 \lambda + 3\omega^2 L_d^4 \alpha^2 (R_s + R_c)\psi_r (1+\alpha) \tag{25}$$

$$Y = L_d^3 \alpha^3 \lambda + L_d^5 \alpha^3 \omega^2 (R_s + R_c) \tag{26}$$

$$Z = -i_{qe}^2 \sigma^2 \psi_r^2 L_d^3 \lambda \omega^2 \alpha \tag{27}$$

where, $\lambda = R_s R_c^2$, $\alpha=(1-\sigma)$ and $\sigma= L_q/L_d$

It is seen from (22)-(27) that i_d^* is function of effective d-q axis components i_{de} and i_{qe}. However, for simplicity in practice, i_{de} and i_{qe} are considered as total i_d and i_q, respectively.

III. Overall Control of the Proposed WECS System

The block diagram of the control structure for the proposed WECS is shown in Fig. 5. The reference speed ω^* is generated based on the developed MPPT algorithm, which is compared with actual speed of IPMSG. The actual speed of the IPMSG is estimated online based on generator terminal voltages and currents using the MRAS based sensorless technique. The speed error is processed through speed controller which gives the q-axis command current i_q^* as output. The d-axis command current i_d^* is generated by the LMA, which controls the air-gap flux of the generator corresponding to the minimum loss condition. The d-q axis command voltages v_d^* and v_q^*, are obtained from d-q axis current controllers, respectively. The PWM signals for generator side controlled rectifier are generated based on space vector modulation. A resistive load is connected across the low pass filter of the DC link. Capacitive bank is connected between IPMSG and controlled rectifier to filter out voltage spikes generated by rectifier.

A. Maximum Power Point Tracking Algorithm

With changing wind speed, rotor speed needs to be

0093-9994 (c) 2015 IEEE. Personal use is permitted, but republication/redistribution requires IEEE permission. See http://www.ieee.org/publications_standards/publications/rights/index.html for more information.

This article has been accepted for publication in a future issue of this journal, but has not been fully edited. Content may change prior to final publication. Citation information: DOI 10.1109/TIA.2015.2510507, IEEE Transactions on Industry Applications

controlled optimally to extract maximum power from it. The proposed MPPT algorithm computes optimum speed based on change in output power direction. It conforms that power curve *(P-ω)* corresponds to $dP/d\omega = 0$ follows the maximum power point as shown in Fig. 6. The flowchart for the proposed MPPT algorithm based on PO method is shown in Fig. 7. The estimated power output P_e is calculated based on sensed I_{abc} and V_{abc}. This power is sampled to check the changes in direction and difference between previous and current values (ΔP_e). ΔP_e is checked if it is within the adequate range, then the optimum speed reference value remains same. The control variable X is considered as rotor

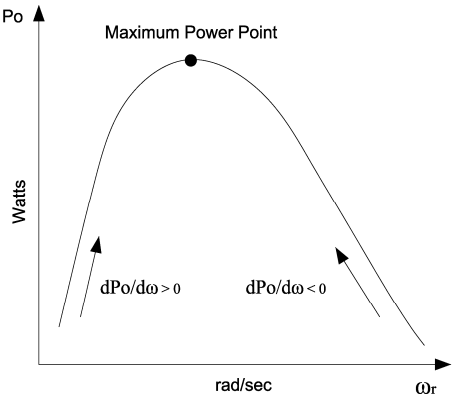

Fig. 6 Hill climb search algorithm for MPPT.

speed for this paper. According to the direction of ΔP_e and ΔX, sign is assigned for optimum step change in speed. The sign is multiplied with ΔPe and variable 'K' to find optimum ΔX. Here, K is a function of X which is designed in such a way that it gives larger value of ΔX at low value of X and vice versa. The following function is developed to adapt the coefficient K with the value of X based on trial and error in simulation so that the MPPT algorithm converges faster.

$$K = -2e^{(-0.0002(X-300)^2)} + 2.01 \quad (28)$$

Optimum speed reference is found by adding ΔX to previous value of X. As shown in Fig. 8 optimum speed is tracked to extract the maximum power at different wind speeds. The curve connecting to A-B-C shows the path of maximum power points.

B. MRAS Based Speed Sensorless Scheme

The model reference adaptive system (MRAS) scheme offers simpler implementation and requires less computational effort as compared to those of other methods, and it is widely accepted for speed estimation [18]. The MRAS method uses two models: one independent of rotor speed (reference model) and the other dependent on rotor speed (adjustable model), both having the same output (back-EMF). The error of these actual and estimated outputs is fed to the adaptation mechanism, which outputs the estimated rotor speed ($\hat{\omega}$) as shown in Fig. 9. This estimated speed is

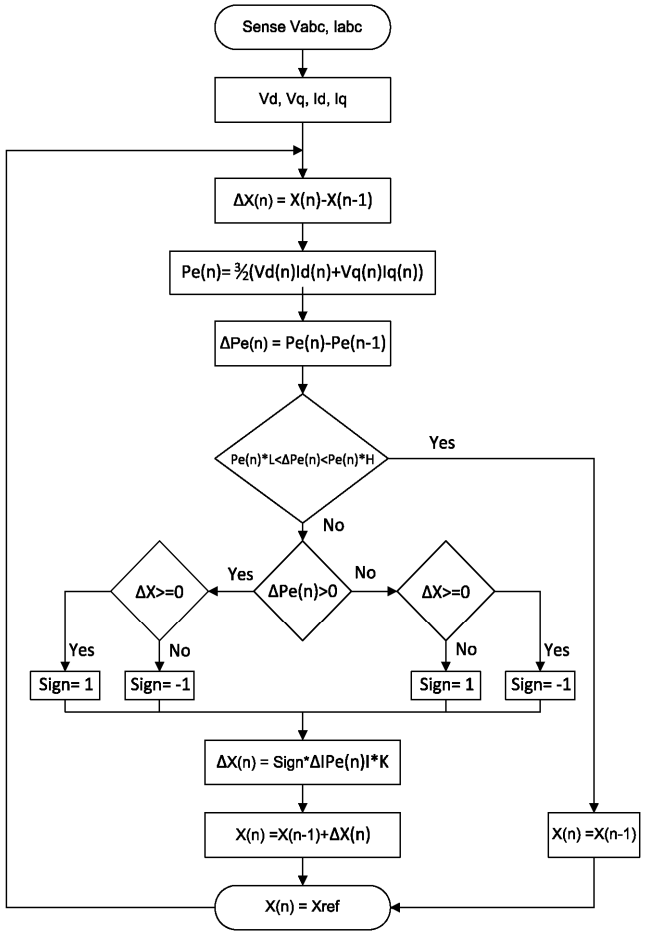

Fig. 7 Flow chart for the proposed MPPT algorithm.

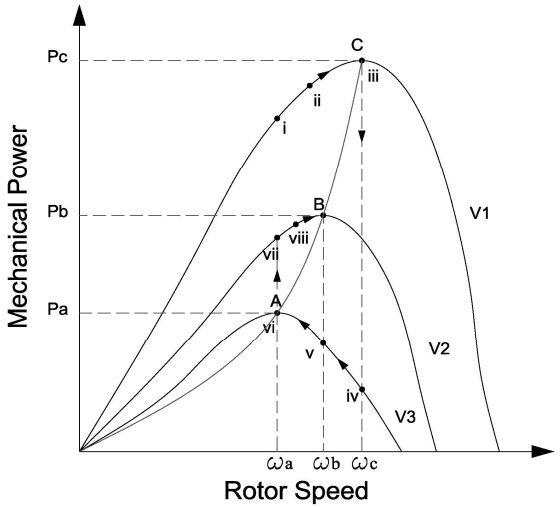

Fig. 8 Change of operating point for MPPT.

used to tune the adjustable model till error is zero at which the estimated speed is same as the actual speed. In Fig. 7 the stator current model with stator current output is used as adaptive model. The error between the actual and estimated output currents is fed to an adaptation mechanism which

0093-9994 (c) 2015 IEEE. Personal use is permitted, but republication/redistribution requires IEEE permission. See http://www.ieee.org/publications_standards/publications/rights/index.html for more information.

This article has been accepted for publication in a future issue of this journal, but has not been fully edited. Content may change prior to final publication. Citation information: DOI 10.1109/TIA.2015.2510507, IEEE Transactions on Industry Applications

could be a PI or sliding mode controller. In d-q reference frame, the mathematical model of IPMSM Eqns. (6-9) can be rewritten in current model form as:

$$p\begin{bmatrix} i_d+\frac{\psi_m}{L_d} \\ i_q \end{bmatrix}=\begin{bmatrix} \frac{-R_s}{L_d} & \omega\frac{L_q}{L_d} \\ -\omega\frac{L_d}{L_q} & \frac{-R_s}{L_q} \end{bmatrix}\begin{bmatrix} i_d+\frac{\psi_m}{L_d} \\ i_q \end{bmatrix}+\begin{bmatrix} \frac{1}{L_d} & 0 \\ 0 & \frac{1}{L_q} \end{bmatrix}\begin{bmatrix} v_d+\frac{R_s\psi_m}{L_d} \\ v_q \end{bmatrix} \quad (29)$$

where, p is derivative operator. Eqn. (29) can be rewritten as,

$$p\begin{bmatrix} i_d+\frac{\psi_m}{L_d} \\ i_q \end{bmatrix}=\begin{bmatrix} \frac{-R_s}{L_d} & \omega\frac{L_q}{L_d} \\ -\omega\frac{L_d}{L_q} & \frac{-R_s}{L_q} \end{bmatrix}\begin{bmatrix} i_d+\frac{\psi_m}{L_d} \\ i_q \end{bmatrix}+\begin{bmatrix} \frac{v_dL_d+R_s\psi_m}{L_d^2} \\ \frac{v_q}{L_q} \end{bmatrix} \quad (30)$$

assuming,

$$x=\begin{bmatrix} x_1 \\ x_2 \end{bmatrix}=\begin{bmatrix} i_d+\frac{\psi_m}{L_d} \\ i_q \end{bmatrix},\ A=\begin{bmatrix} \frac{-R_s}{L_d} & \omega\frac{L_q}{L_d} \\ -\omega\frac{L_d}{L_q} & \frac{-R_s}{L_q} \end{bmatrix},\ u=\begin{bmatrix} \frac{v_dL_d+R_s\psi_m}{L_d^2} \\ \frac{v_q}{L_q} \end{bmatrix}$$

Thus, the state Eqn. (30) can rewritten as,

$$px=Ax+u \quad (31)$$

So the adaptive model can be written as,

$$p\hat{x}=A\hat{x}+u \quad (32)$$

where, $\hat{A}=\begin{bmatrix} \frac{-R_s}{L_d} & \hat{\omega}\frac{L_q}{L_d} \\ -\hat{\omega}\frac{L_d}{L_q} & \frac{-R_s}{L_q} \end{bmatrix}$, and $\hat{x}$ is the estimated value of the parameter x. The error vector is given by,

$$e=x-\hat{x}=\begin{bmatrix} x_1-\hat{x}_1 \\ x_2-\hat{x}_2 \end{bmatrix} \quad (33)$$

From Eqns. (31) and (32), there would be,

$$pe=Ae-H \quad (34)$$

where, $H=(\hat{\omega}-\omega)=\begin{bmatrix} 0 & \frac{L_q}{L_d} \\ -\frac{L_d}{L_q} & 0 \end{bmatrix}\hat{x}$ According to Popov's hyperstability criterion the adaptive law can be obtained as [26-28]:

$$\hat{\omega}=C_1(N)+C_2\int(N)d\tau+\hat{\omega}(0) \quad (35)$$

$$\hat{\theta}=\int(\hat{\omega})d\tau \quad (36)$$

where, $N=-\frac{L_d}{L_q}\left(\hat{i}_d+\frac{\psi_m}{L_d}\right)\left(i_q-\hat{i}_q\right)+-\frac{L_q}{L_d}\hat{i}_q\left(i_d-\hat{i}_d\right)$, $\hat{\omega}(0)$ is the initial speed and C_1, C_2 are proportional and integral gains, respectively. The gains of this adaptation mechanism are calculated through Popov's hyperstability criterion. Eqn. (35) represents a PI controller. Thus, the error between reference and adaptive model is processed through a PI controller, which gives the estimated speed of the generator. The estimating performance of the rotor speed is optimized by adjusting the PI coefficients through trial and error procedure. In this work the PI gains were selected as 0.8 and 0.5, respectively. The actual 3-phase currents are measured and then converted to d-q components. The current error model is generated based on these currents and the reference currents obtained from MPPT and speed controller, respectively.

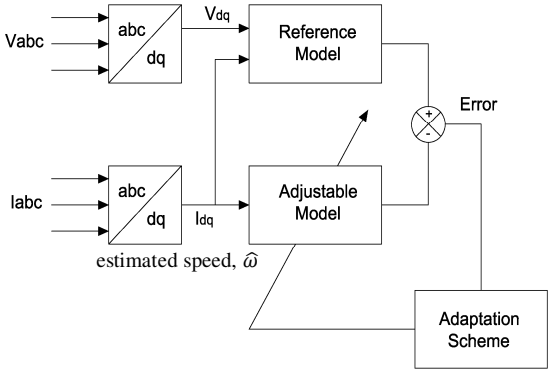

Fig. 9 Model reference adaptive system for speed estimation.

IV. Results And Discussions

A. Simulation Results

The performance of the proposed adaptive MPPT control of IPMSG incorporating the LMA and speed sensorless schemes for wind energy conversion system is investigated extensively in simulation using MATLAB/Simulink software. The wind turbine is modeled based on Eqns. (1)-(4). The parameters for IPMSG used in simulation are given in Appendix. Please note that the parameter used in the MPPT, LMA and MRAS algorithms are considered constant at nominal values for the sake of testing the proposed algorithms. An online parameter estimation algorithm may be used to update the parameters online so that magnetic saturation or other system disturbances and nonlinearities can be included [30]. However, the performance of the proposed adaptive MPPT based WECS is compared with the conventional MPPT based WECS. Sample results are presented below.

Figure 10 shows the responses of the proposed WECS incorporating the MPPT, LMA and sensorless based control of IPMSG for step changes in wind speed. It is seen from Fig. 10(a) that the turbine torque follows smoothly according to the disturbances in wind speed. Fig. 10(b) shows that the proposed MRAS based sensorless scheme can estimate the generator rotor speed smoothly according to the changes in wind speed. It is seen from Fig. 10(c) that there is not much difference between turbine power and dc-link power, which indicates that the LMA and MPPT algorithms work

0093-9994 (c) 2015 IEEE. Personal use is permitted, but republication/redistribution requires IEEE permission. See http://www.ieee.org/publications_standards/publications/rights/index.html for more information.

This article has been accepted for publication in a future issue of this journal, but has not been fully edited. Content may change prior to final publication. Citation information: DOI 10.1109/TIA.2015.2510507, IEEE Transactions on Industry Applications

effectively. This fact is also proved by the efficiency response of WECS presented in Fig. 10(d). The WECS efficiency is calculated as a ratio of mechanical output power of turbine, P_m to dc-link output power, P_o. It is seen that the proposed system can maintain almost constant efficiency of around 87% in spite of the wind variation from 7m/s to 17 m/s. Fig. 11 shows the comparative mechanical power output of wind turbine, P_m and dc-link output power, P_o for the proposed and conventional MPPT based WECS. It is clearly see from this figure that both the turbine power and dc-link power for the proposed adaptive MPPT control system is higher than those of the conventional MPPT based WECS. In conventional MPPT control the optimum torque, T_{opt} of the IPMSG is found from (37), which is a function of WT mechanical parameters and the optimum value of C_p, $C_{p\text{-}opt}$ [31]. Generally, it is considered constant to extract maximum power for specific WT, which was 0.4655 for this paper. Thus, it verifies the effectiveness of proposed MPPT for transferring more power to the dc-link from wind especially, at high wind speed condition.

$$T_{opt} = \frac{\pi}{2}\rho C_{p\_opt}\frac{R^5 {\omega_r}^2}{{\lambda_{opt}}^3} \tag{37}$$

$$i_q^* = \frac{\frac{2}{3P}T_{opt}}{\psi_m + (L_d - L_q)i_d} \tag{38}$$

Fig. 12 shows the zoom-in view of the steady-state 3-phase stator voltages, currents and estimated rotor position corresponding to the step changes in wind speeds. The balanced operation of the generator is verified by the voltages and current waveforms. Fig. 12(c) shows that the estimated rotor position (electrical) matches with the stator 'a' phase current exactly which further verifies the effectiveness of the sensorless algorithm. Figure 13 shows the response of proposed WECS for a real wind speed model as per Eqn.(5). As shown in Fig. 13(a) wind speed varies from 9 m/s to 15 m/s and the turbine torque follows the wind speed variation smoothly. If the wind speed increases the torque also increases and vice versa. Fig. 13(b) shows the estimated and actual rotor speed of the IPMSG. It is clearly seen from Fig. 13 that the high accuracy of rotor speed estimation is maintained over a wide range of wind speed. Fig. 13(c) shows that the output dc-link power follows the mechanical power available from turbine efficiently. To verify the maximum power point tracking operation, the C_p graph is shown in Fig. 13(d), which remains almost constant around 0.46 for the wind profile as shown in Fig. 10(a). As mentioned earlier, the maximum C_p that can be achieved by the proposed system is 0.465 and it is the only controllable variable to extract the maximum power. Fig. 13(e) shows estimation error between estimated and actual rotor speeds. It is seen that the sensorless control scheme can maintain the speed error almost zero except the transient conditions.

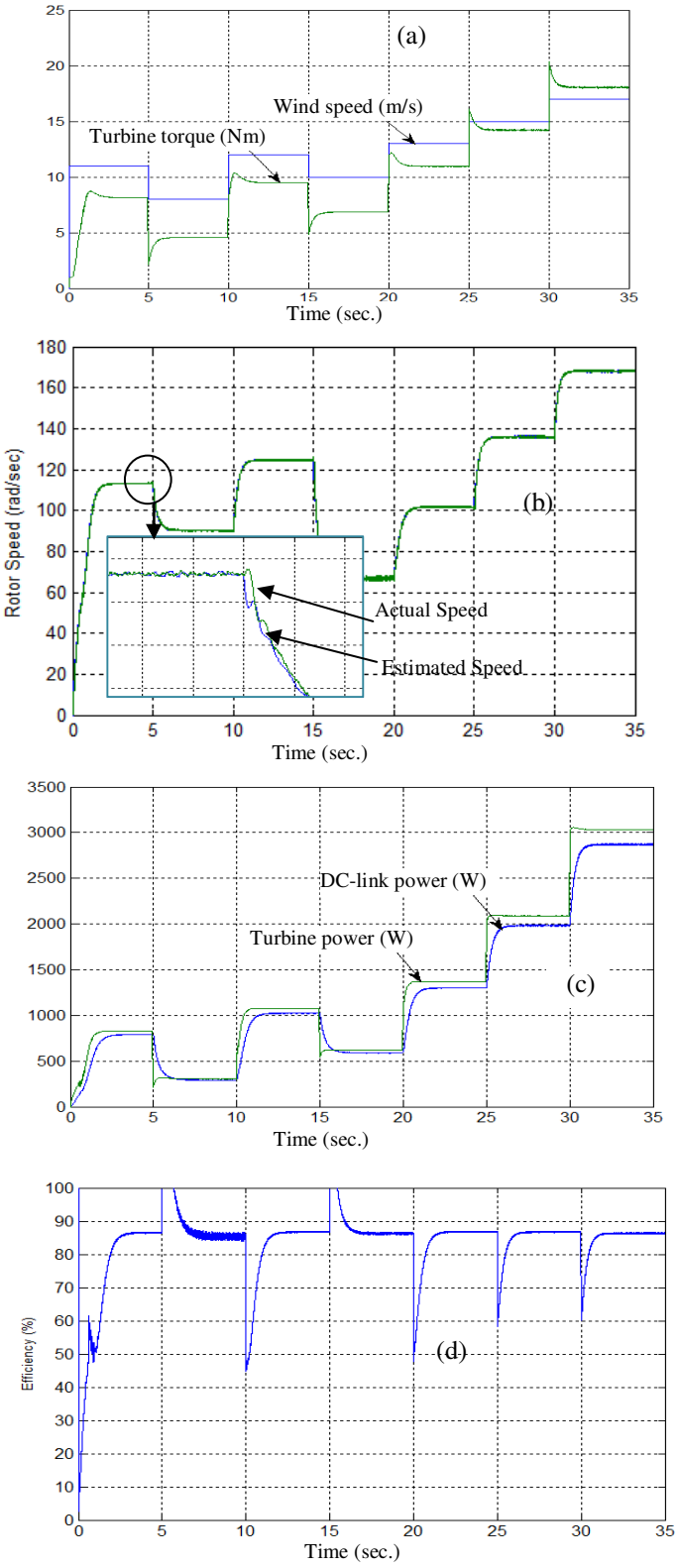

Fig. 10 Responses of the proposed IPMSG based WECS for step changes of wind speed: (a) Wind speed (m/s) and Turbine torque (Nm) (b) Rotor actual and estimated speed (rad/s) (c) Turbine power P_m and dc-link power P_o (W) , and (d) Efficiency (η).

0093-9994 (c) 2015 IEEE. Personal use is permitted, but republication/redistribution requires IEEE permission. See http://www.ieee.org/publications_standards/publications/rights/index.html for more information.

This article has been accepted for publication in a future issue of this journal, but has not been fully edited. Content may change prior to final publication. Citation information: DOI 10.1109/TIA.2015.2510507, IEEE Transactions on Industry Applications

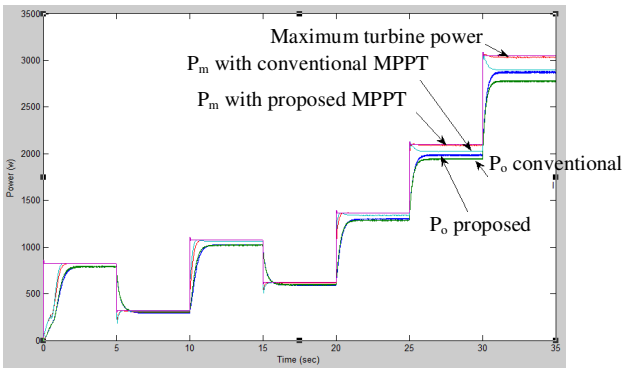

Fig. 11 Power extraction for the proposed and conventional MPPT based WECS with step changes in wind speed shown in Fig. 8(a).

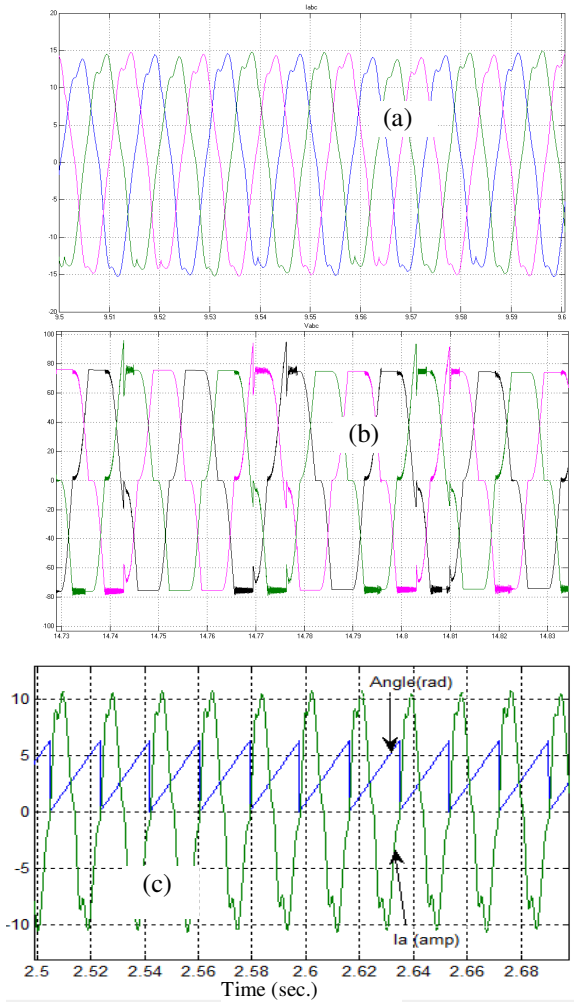

Fig. 12 Zoom-in view for a step changes in wind speed: (a) 3-phase stator currents, (b) 3-phase stator voltages, and (c) 'a' phase current and estimated rotor position.

B. Experimental Results

The proposed adaptive MPPT control of IPMSG incorporating the LMA and speed sensorless schemes for WECS is experimentally implemented using DSP board DS1104 [32]. The experimental setup for the prototype 5 hp IPMSG based WECS is shown in Fig. 14. The test IPMSG is labelled as 'G'. The rotor speed of the test machine is measured by an optical incremental encoder which is labelled as 'E'. The measured speed is only used for comparison purpose with the estimated rotor speed. The IPMSG is coupled with a PM-DC machine (M), which works as a separately excited motor to drive the generator. Thus, the DC motor replaces the wind turbine in a laboratory environment. The actual motor currents are measured by Hall-effect current transducers. The interface circuit (I) is located between the Hall-effect sensor (CS) and the A/D channel of DSP board DS1104. The DSP board is installed in a personal computer (PC). A gate drive circuit (D) is used to increase the power level of the firing pulses so that these are sufficient to drive the insulated gate bipolar transistor (IGBT) switches of the converter. The power circuits consist of a 3-phase variable autotransformer (A), power supply (PS), rectifier (R) and IGBT converter (V). The ac voltage is supplied by the power supply through autotransformer which is rectified by a 3-phase uncontrolled rectifier (R) to supply DC motor. The speed of the motor is changed by varying the input ac voltage to the rectifier. Thus, it simulates the variable wind speed conditions. A digital storage oscilloscope (O) is used to capture the desired analog signal coming out through D/A port of the DSP board. Sample results are presented below.

Fig. 15 shows the effectiveness of the speed sensorless scheme under variable speed conditions. It can be seen that the estimated speed tracks the actual rotor speed very well. As the IPMSG is 3 pole pair machine, one cycle of rotor position angle corresponds to three cycle of phase 'a' current, which is shown in Fig. 16. The balanced operation of the generator is verified by the steady-state three phase output voltages, which are shown in Fig. 17. The effectiveness of the MPPT and LMA algorithms can be seen from Fig. 18, which shows that the proposed MPPT and LMA can transfer more power to the dc-link as compared to the conventional MPPT based WECS. For conventional MPPT control in real-time the turbine output power is first estimated based on simulation results at different speed and load conditions and then the reference speed for the wind generator is calculated. After that the same PI speed controller was utilized to generate the torque component of the current, i_q. Thus, in conventional control electrical load variation was not sensed by the controller and hence, the maximum power transfer was not ensured. Due to limitation of the variable dc power supply it was possible to run the motor up to 70 rad/s. It was found that the proposed LMA based MPPT can maintain the efficiency of around 85%, which is almost similar to the simulation results. As the IPMSG is driven by 5 hp PM DC motor in a laboratory environment, the WT parameter is unavailable for conventional controller. This is also the limitation of the conventional MPPT control of WECS in real-time.

0093-9994 (c) 2015 IEEE. Personal use is permitted, but republication/redistribution requires IEEE permission. See http://www.ieee.org/publications_standards/publications/rights/index.html for more information.

This article has been accepted for publication in a future issue of this journal, but has not been fully edited. Content may change prior to final publication. Citation information: DOI 10.1109/TIA.2015.2510507, IEEE Transactions on Industry Applications

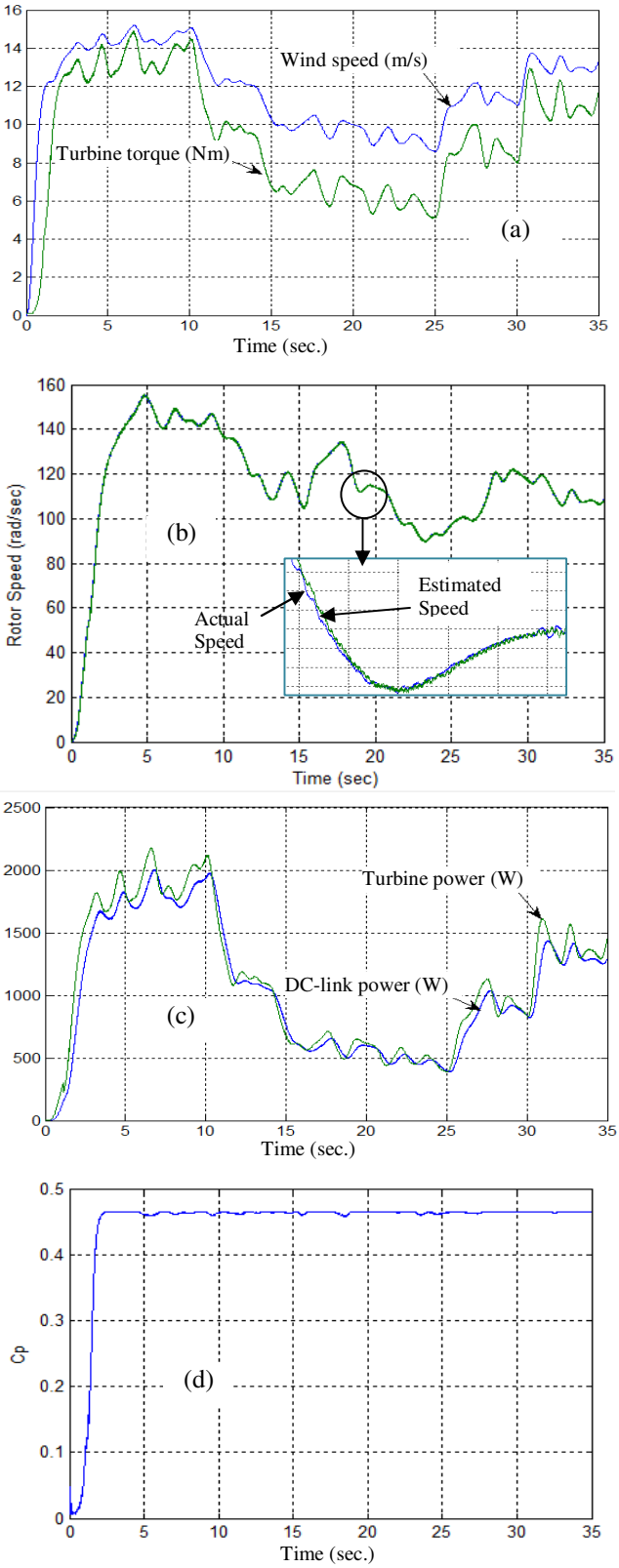

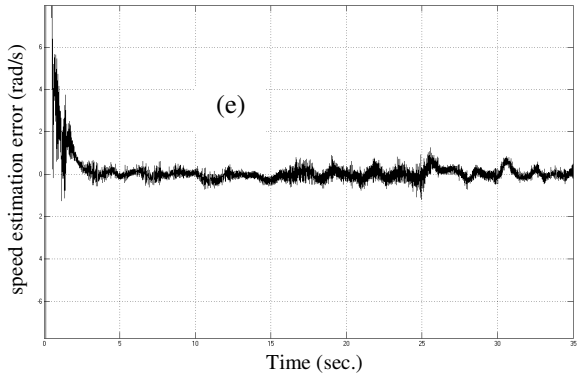

Fig. 13 Responses of the proposed IPMSG based WECS for real wind speed model: (a) wind speed (m/s) and turbine torque (Nm), (b) rotor speed (rad/s) and, (c) turbine power, P_m (W) and output DC link power, P_o (W), (d) wind turbine power coefficient, C_p, and (e) speed estimation error.

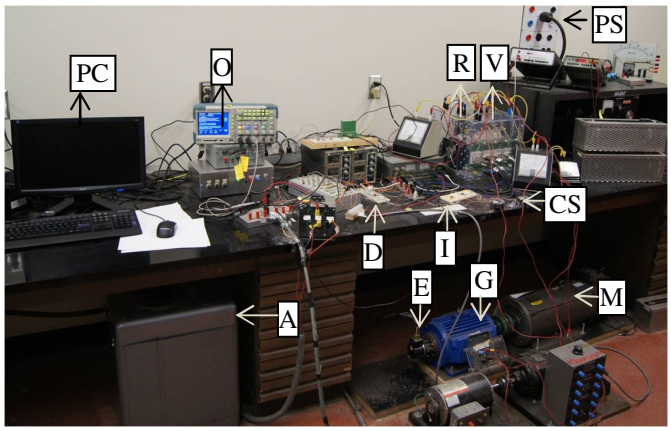

Fig.14 Experimental setup of the proposed IPMSG based WECS (DC motor replaces the wind turbine in the lab).

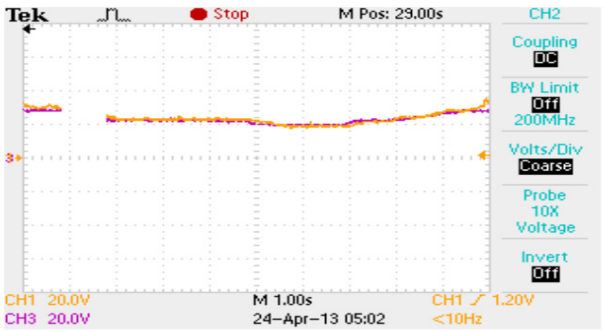

Fig. 15 Measured and estimated rotor speed of the generator.

0093-9994 (c) 2015 IEEE. Personal use is permitted, but republication/redistribution requires IEEE permission. See http://www.ieee.org/publications_standards/publications/rights/index.html for more information.

This article has been accepted for publication in a future issue of this journal, but has not been fully edited. Content may change prior to final publication. Citation information: DOI 10.1109/TIA.2015.2510507, IEEE Transactions on Industry Applications

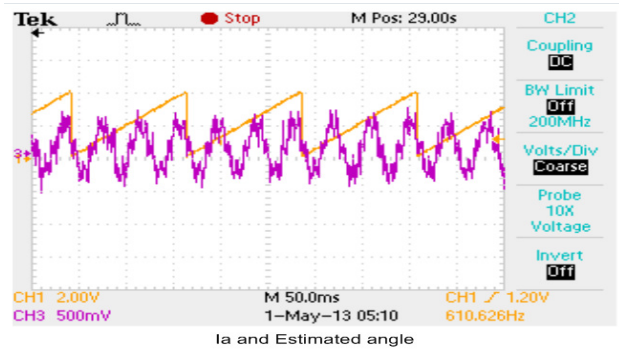

Fig. 16 Steady-state 'a' phase current and rotor position of the generator.

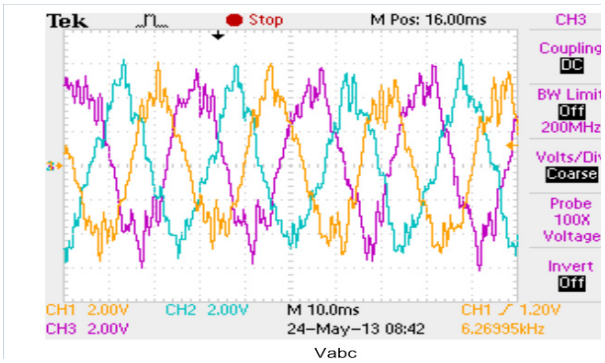

Fig. 17 Steady-state 3-phase stator currents of the generator.

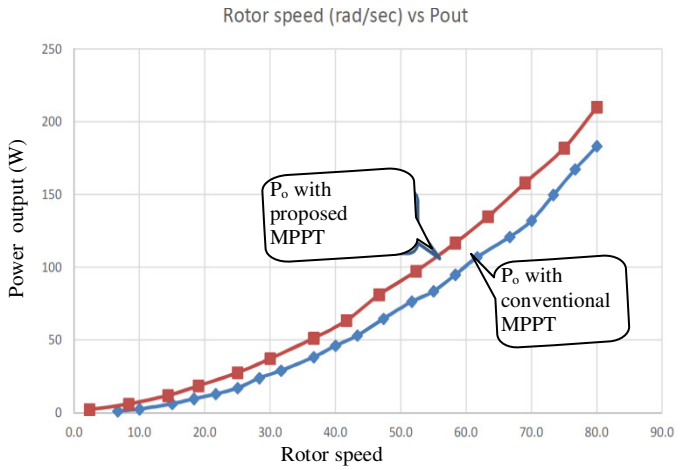

Fig. 18 DC-link output power, P_o at different speeds (rad/s) with the proposed and conventional MPPT algorithms.

V. Conclusion

A speed sensorless and loss minimization based adaptive MPPT operation of IPMSG for direct-drive wind energy conversion system has been presented in this paper. A simple model reference adaptive system was utilized to estimate the rotor position. A novel online adaptive MPPT operation was utilized to transfer maximum power from wind turbine to the dc-link. A model based LMA has also been incorporated to minimize the electrical losses of the generator. The MPPT algorithm generates the optimum reference speed of the generator without the knowledge of wind speed, turbine or generator parameters. The proposed control technique was implemented in real-time using DSP board DS1104 for a laboratory 5 hp IPMSG. The effectiveness of the proposed speed sensorless and LMA based MPPT control of IPMSG was verified in both simulation and experiment. It was found that the proposed control techniques can transfer maximum power while maintaining accurate speed estimation of the generator at different wind speed conditions. The MPPT operation was confirmed by maintaining maximum C_p and high controllability of the IPMSG. Therefore, the proposed speed sensorless and LMA based adaptive MPPT scheme could be a potential candidate for reliable operation of industrial wind energy conversion systems.

Appendix: IPMSG Parameters

Rated Power	5 hp
Number of poles	6
Number of phases	3
q-axis inductance, L_q	6.42 mH
d-axis inductance, L_d	5.06 mH
Stator resistance R_s	0.242 ohm
Core loss resistance R_c	7.5 ohm
Inertia constant J	0.0133 kg.m^2
Damping constant B_m	0.001 (Nm)/rad/sec
PM flux linkage ψ_m	0.24 volts/rad/sec

ACKNOWLEDGEMENT: This work was supported by the Natural Science and Engineering Research Council (NSERC), Canada under the Discovery Grants-Individual program.

VI. References

[1] S. Morimoto, H. Kato, M. Sanada and Y. Takeda, "Output Maximization Control for Wind Generation System with Interior Permanent Magnet Synchronous Generator," IEEE IAS Annual Meeting, 2006, pp. 1-8. S.

[2] Morimoto, M. Sanada and Y. Takeda, "Optimum control of IPMSG for wind generation system," Osaka Power Conversion Conference, Osaka, August 2002.

[3] J. S. Thongam, P. Bouchard, H. Ezzaidi and M. Ouhrouche, "Wind Speed Sensorless Maximum Power Point Tracking Control of Variable Speed Wind Energy Conversion Systems," IEEE IEMDC, Miami, FL, May 2009, pp. 1832-1837.

[4] N. Srighakollapu and P. Sensarma, "Sensorless maximum power point tracking control in wind energy generation using permanent magnet synchronous generator," in 34th Annual Conference of IEEE Industrial Electronics, Orlando, FL, 10-13 Nov. 2008.

[5] J. S. Thongam, P. Bouchard, R. Beguenane and I. Fofana, "Neural network based wind speed sensorless MPPT controller for variable speed wind energy conversion systems," in IEEE Electric Power and Energy Conference, Halifax, NS, Aug 25-27, 2010.

[6] Blaabjerg, F.; Ke Ma, "Future on Power Electronics for Wind Turbine Systems," Emerging and Selected Topics in Power Electronics, IEEE Journal of , vol.1, no.3, pp.139,152, Sept. 2013.

[7] A. M. O. Haruni, M. E. Haque, A. Gargoom and M. Negnevitsky, "Control of a Direct Drive IPM Synchronous Generator Based Variable

0093-9994 (c) 2015 IEEE. Personal use is permitted, but republication/redistribution requires IEEE permission. See http://www.ieee.org/publications_standards/publications/rights/index.html for more information.

This article has been accepted for publication in a future issue of this journal, but has not been fully edited. Content may change prior to final publication. Citation information: DOI 10.1109/TIA.2015.2510507, IEEE Transactions on Industry Applications

Speed Wind Turbine with Energy Storage," IEEE IECON Conference, Glendale, AZ, Nov 2010.
[8] M. Nasir Uddin, and J. Khastoo, "Fuzzy Logic Based Efficiency Optimization and Improvement of Dynamic Performance of IPM Synchronous Motor Drive", IEEE Trans. on Ind. Applications, vol. 50, no.6, Nov./Dec. 2014, pp. 4251-4259.
[9] W. Qiao, L. Qu and R. G. Harley, "Control of IPM Synchronous Generator for Maximum Wind Power Generation Considering Magnetic Saturation," IEEE Trans. on Ind. Application , vol 45, no. 3, May- June 2009, pp. 1095-1105.
[10] A.M. De Broe, S. Drouilhet, V. Gevorgian, "A peak power tracker for small wind turbines in battery charging applications," IEEE Trans. on Energy Conversion, vol. 14, no. 4, Dec. 1999, pp. 1630-1635.
[11] M. Chinchilla, S. Arnaltes, and J.C. Burgos, "Control of Permanent Magnet Generators Applied to Variable-Speed Wind-Energy Systems Connected to the Grid", IEEE Trans. on Energy Conv., vol. 21, no. 1, Mar. 2006, pp. 130-135.
[12] W. Liu, L. Chen, J. Ou and S. Cheng, "Simulation of PMSG wind turbine system with sensorless control technology based on model reference adaptive system," International Conference on Electrical Machines and Systems, Beijing, China, 2011, pp.1-3.
[13] B. Boukhezzar and H. Siguerdidjane, "Nonlinear control of variable speed wind turbines without wind speed measurement," in Proc. 44th IEEE Conference on Decision and Control, Seville, Spain, Dec. 12-15, 2005, pp. 3456-3461.
[14] X. Gong, X. Yang and W. Qiao, "Wind Speed and Rotor Position Sensorless Control for Direct Drive PMG Wind Turbines," IEEE Trans. on Ind. Applications, vol. 48, no. 1, , Jan.-Feb. 2012 pp. 3- 11.
[15] X. Yang, X. Gong, & W. Qiao, "Mechanical sensorless maximum power tracking control for direct-drive PMSG wind turbines", IEEE ECCE Conference, 2010, Atlanta, USA, pp. 4091- 4098.
[16] Y. Kano, T. Kosaka, N. Matsui, T. Takahashi, M. Fujitsuna, "Signal-injection-based sensorless IPM traction drive for wide-torque range operation at low speed", IEEE Energy Conversion Congress and Exposition (ECCE), Sept. 2012, pp.2284-2291.
[17] O. Benjak, D. Gerling, "Review of position estimation methods for IPMSM drives without a position sensor Part- I and Part-II: Nonadaptive methods," Int. Conf. on Electrical Machines (ICEM), Sept. 2010.
[18] Z. Xingming, W. Xuhui, Z. Feng; G. Xinhua, and Z. Peng, "Wide-speed-range sensorless control of Interior PMSM based on MRAS," International Conference on Electrical Machines and Systems (ICEMS), Oct. 2010, vol.10, no.13, pp.804-808.
[20] H. M. Kojabadi, and M. Ghribi, "MRAS-based adaptive speed estimator in PMSM drives," Proceedings of Advanced Motion Control Conference, Istanbul, Turkey, March 2006, pp. 569–572.
[21] K. Huang; W. Li, Shoudao Huang; L. Xiao; L. Zheng; Z. Xu, "Sensorless control of direct-driven permanent magnet wind power generation system based on improved MRAS," Int. Conf. on Electrical Machines and Systems (ICEMS), 2011, vol.20, no.23, pp.1-5.
[22] R. Cardenas, R. Pena, J. Proboste, G. Asher, and J. Clare, "MRAS observer for sensorless control of standalone doubly fed induction generators, vol. 20 , no. 4, Dec. 2005, pp. 710 – 718.
[23] M. Nasir Uddin, and R. Rebeiro, "Online Efficiency Optimization of a Fuzzy-Logic-Controller-Based IPMSM Drive," Industry Applications, IEEE Transactions on , vol.47, no.2, pp.1043-1050, March-April 2011.
[24] M. Nasir Uddin, and J. Khastoo, "Fuzzy Logic Based Efficiency Optimization and Improvement of Dynamic Performance of IPM Synchronous Motor Drive", IEEE Trans. on Ind. Applications, vol. 50, no. 06, Nov./Dec. 2014, pp. 4251 - 4259.
[25] M. Nasir Uddin and S. Nam, "New On-line Loss Minimization Based Control of an Induction Motor Drive", IEEE Trans. on Power Electronics, Vol. 23, No.2, March 2008, pp. 926-933.
[26] V. T. Buyukdegirmenci, A. M. Bazzi and P. T. Krein, "Evaluation of Induction and Permanent Magnet Synchronous Machines Using Drive-Cycle Energy and Loss Minimization in Traction Applications", *IEEE Trans. Ind. Appl.,* vol. 50, no.1, Jan. 2014, pp.395-403.
[27] V. M. Popov, *Stability Spaces and frequency-domain conditions in Calculus of variations and control*, Academic Press New York-san Francisco, London, 1976, pp. 371-390.
[28] I. Landau, A hyperstability criterion for model reference adaptive control systems, , IEEE Trans. on Automatic Control, vol.14, no.5, , Oct 1969, pp. 552-555.
[29] P. M. Anderson and A. Bose., "Stability Simulation Of Wind Turbine Systems", IEEE Trans. on Power Apparatus and Systems, vol. 102, no.12, Dec. 1983, pp.3791-3795.
[30] M. Nasir Uddin and M. I. Chy, "On-Line Parameter Estimation Based Speed Control of PM AC Motor Drive in Flux Weakening Region", IEEE Trans. on Ind. Applications, Vol. 44, No. 5, Sept./Oct. 2008, pp. 1486-1494.
[31] H. Camblog, I. M. de Alegria, M. Rodriguez, and G. Abab, "Experimental evaluation of wind turbines maximum power point tracking controllers" Energy Conversion Management, vol. 47, no 18-19, pp.2846-2858, 2006.
[32] dSPACE, DSP (DS1104) Manual Guide, Paderborn, Germany, 2007.

Author's Biography:

M. Nasir Uddin received the B.Sc. and M. Sc. degrees both in electrical & electronic engineering from Bangladesh University of Engineering and Technology (BUET), Dhaka, Bangladesh, and the Ph.D. degree in electrical engineering from Memorial University of Newfoundland (MUN), Canada in 1993, 1996, and 2000, respectively.

He has been serving as a Professor in the Department of Electrical Engineering, Lakehead University (LU), Thunder Bay, ON, Canada since August 2001. He also served as a visiting Prof. at Univ. of Malaya (2013, 2012, 2011), Tokyo University of Science (2010), Japan and North South University (2006), Dhaka, Bangladesh. Previously, he was an Assistant Professor in the Department of Electrical and Computer Engineering, University of South Alabama, USA from January 2001 to May 2001, an Assistant Professor from 1996 to 1997 and a lecturer from 1994 to 1996 at BUET. He possesses more than 20 years of teaching experience and has authored/coauthored over 180 papers in international journals (32 in IEEE Transactions) and conferences.

Prof. Uddin is a Registered Professional Engineer in the Province of Ontario, Canada. He served as one of the Technical Program Committee Chairs for IEEE Energy Conversion Congress and Expo (ECCE) 2015 at Montreal, Canada. He was the Technical Committee Chair for the IEEE Industry Applications Society (IAS) [Industrial Automation and Control Committee (IACC)] Annual Meetings in 2011 and 2012. He served as Papers Review Chair (2009–2010 and 2013–2014) of the IEEE Transactions on Industry Applications (IACC). He is elected to serve as IEEE IAS Executive Board member and chair of IAS Manufacturing Systems Development and Applications Department for 2016-2017. Earlier he served IEEE IAS IACC for 9 years in different capacities. Due to his outstanding contributions IEEE IAS IACC recognized him with IEEE IAS Service Award 2015. He also received LU Distinguished Researcher Award 2010. He was the recipient of two First Prize, one 2nd Prize and one Third Prize Paper Awards from IEEE IAS IACC and both 2004 Contributions to Research and Contributions to Teaching Awards from LU. His research interests include power electronics, renewable energy, motor drives, and intelligent controller applications.

Nirav Patel received his B.Sc. in Electrical Engineering and M.Sc. Control Engineering both from Lakehead University, Thunder Bay, ON, Canada in 2011 and 2013, respectively. Currently, he is working as an electronics test specialist at Gentherm, ON, Canada. His research interests are in the area of renewable energy systems, wind turbine control systems, and power electronics. Mr. Nirav received the IEEE Industry Applications Society (IAS) Myron Zucker Student Design Contest Award (3rd Prize) 2011 for Dual Rotor Maglev Axial Flux Generator design.

0093-9994 (c) 2015 IEEE. Personal use is permitted, but republication/redistribution requires IEEE permission. See http://www.ieee.org/publications_standards/publications/rights/index.html for more information.